Accepted Manuscript

2,4,5-Trisubstituted thiazole derivatives as HIV-1 NNRTIs effective on both wild-type and mutant HIV-1 reverse transcriptase: Optimization of the substitution of positions 4 and 5

Zhongliang Xu, Jiamei Guo, Ying Yang, Mengdi Zhang, Mingyu Ba, Zhenzhong Li, Yingli Cao, Ricai He, Miao Yu, Hua Zhou, Xiaoxi Li, Xiaoshan Huang, Ying Guo, Changbin Guo

PII: S0223-5234(16)30608-0

DOI: 10.1016/j.ejmech.2016.07.047

Reference: EJMECH 8765

To appear in: *European Journal of Medicinal Chemistry*

Received Date: 7 March 2016

Revised Date: 19 July 2016

Accepted Date: 20 July 2016

Please cite this article as: Z. Xu, J. Guo, Y. Yang, M. Zhang, M. Ba, Z. Li, Y. Cao, R. He, M. Yu, H. Zhou, X. Li, X. Huang, Y. Guo, C. Guo, 2,4,5-Trisubstituted thiazole derivatives as HIV-1 NNRTIs effective on both wild-type and mutant HIV-1 reverse transcriptase: Optimization of the substitution of positions 4 and 5, *European Journal of Medicinal Chemistry* (2016), doi: 10.1016/j.ejmech.2016.07.047.

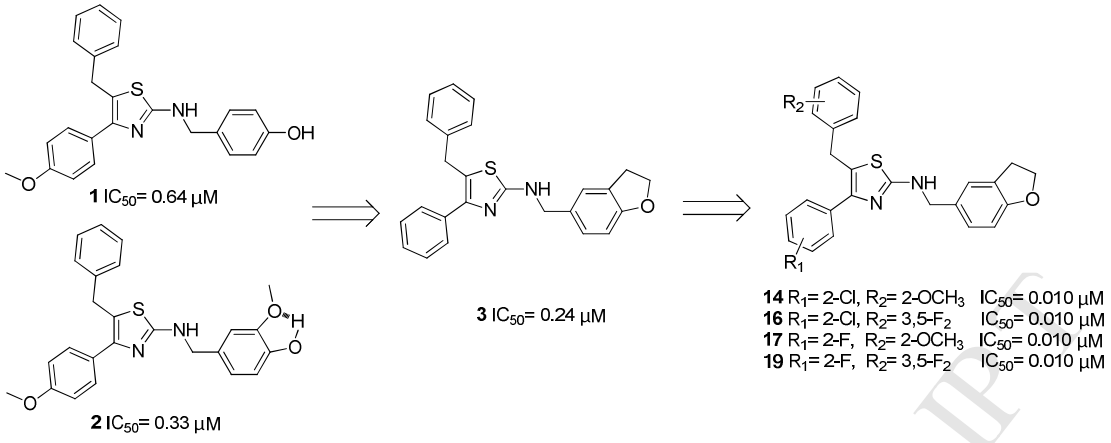

2,4,5-Trisubstituted Thiazole Derivatives as HIV-1 NNRTIs Effective on Both Wild-Type and Mutant HIV-1 Reverse Transcriptase: Optimization of the Substitution of Positions 4 and 5

Zhongliang Xu[a,1], Jiamei Guo[b,1], Ying Yang[b,1], Mengdi Zhang[a], Mingyu Ba[b], Zhenzhong Li[a], Yingli Cao[b], Ricai He[a], Miao Yu[b], Hua Zhou[a], Xiaoxi Li[a], Xiaoshan Huang[a], Ying Guo[b,*], Changbin Guo[a,*]

[a] Department of Chemistry, Capital Normal University, Beijing, 100048, China.

[b] State Key Laboratory of Bioactive Substance and Function of Natural Medicines, Institute of Materia Medica, Chinese Academy of Medical Sciences and Peking Union Medical College, Beijing, 100050, China

Corresponding Authors

Phone, +86-10-68902249; *E-mail*, guocb@cnu.edu.cn (G.CB.). Phone, +86-10-63161716; *E-mail*, yingguo6@imm.ac.cn (G.Y.).

[1] Authors Zhongliang Xu, Jiamei Guo, and Ying Yang contributed equally.

List of abbreviations: RT, reverse transcriptase; NNRTIs, non-nucleoside reverse transcriptase inhibitors; TSTs, 2,4,5-trisubstituted thiazole derivatives; DMSO, dimethyl sulfoxide; VSVG, vesicular stomatitis virus G protein.

Highlights:

1. Twenty-one novel 2,4,5-trisubstituted thiazoles were designed and synthesized.

2. Reasonable design and combination of optimal substituents resulted in increased activity.

3. SAR exploration focused on positions 4 and 5 of the thiazole ring.

4. Some compounds showed inhibition against WT and some mutant viruses.

Keywords: HIV-1, non-nucleoside reverse transcriptase inhibitors, 2,4,5-trisubstituted thiazole derivatives, structure optimization, structure activity relationship.

ABSTRACT: In our previous work, novel 2,4,5-trisubstituted thiazole derivatives (TSTs) were synthesized, and their activities were evaluated against HIV-1 reverse transcriptase. Some interesting results were obtained, which led us to a new discovery regarding these TSTs. In the present study, 21 new 2,4,5-trisubstituted thiazole derivatives were rationally designed and synthesized as HIV-1 non-nucleoside reverse transcriptase inhibitors (NNRTIs) in accordance with our previous study. Among the synthesized target compounds, compounds **14**, **16**, **17**, and **19** showed more potent inhibitory activity against HIV-1 NNRT with an IC_{50} value of 0.010 μM. Compounds **4**, **9**, **10**, **11, 13** and **16** were further tested on nine NNRTI-resistant HIV-1 strains, and all of these compounds exhibited inhibitory effects. A molecular docking study was conducted, and the results showed a consistent and stable binding mode for the typical compounds. These results have provided deeper insights and SAR of these types of NNRTIs.

Introduction

Highly active antiretroviral therapy (HAART) consists of three drugs to sufficiently control HIV infection and restore human immune system functions. Although HAART has significantly improved the treatment of HIV/AIDS [1-4], the emergence of resistance to antiretroviral agents and serious side effects cause widespread failures in the treatment of HIV/AIDS. Therefore, the discovery and development of new drugs should target potent efficacy against resistant viruses and safety properties.

HIV reverse transcriptase (RT) is an enzyme that is essential for viral replication; this enzyme converts the viral single-stranded RNA genome into a double-stranded DNA [5]. RT is a multifunctional enzyme that possesses three activities: RNA-dependent DNA polymerase, DNA-dependent DNA polymerase and ribonuclease H (RNase H) activities [6]. There are two classes of RT inhibitors, namely,

nucleoside reverse transcriptase inhibitors (NRTIs) and non-nucleoside reverse transcriptase inhibitors (NNRTIs), which block DNA polymerase activity and prevent synthesis of the double-stranded DNA [7,8]. NNRTIs are crucial components in HAART due to their unique antiviral efficacy, high specificity and low toxicity characteristics.[9-11] Five NNRTIs have currently been approved by the FDA and have become the cornerstone of HIV/AIDS treatment. Nevertheless, drug resistance is still the main reason for clinical treatment failures [12-14]. NNRTIs can effectively inhibit wild-type HIV replication, but the long-term use of these NNRTIs has led to the generation of resistant viruses, such as RT-K103N and RT-Y181C, which are the most prevalent mutations in clinical HIV-1 isolates and have high-level resistance to current NNRTIs [15]. Therefore, innovative NNRTIs with a higher genetic barrier against clinically relevant mutant strains are still needed [16,17**].**

In our previous work, 2,4,5-trisubstituted thiazole derivatives (TSTs) were first reported as a novel class of NNRTIs against both wild-type and resistant HIV-1, and the IC_{50} of the most active of these compounds is 0.046 μM [18]. The activity apparently increased when compound **1** transformed to compound **2** (Figure 1), which led us to hypothesize that the pseudo 5-membered ring formed by the hydrogen bond between '-OH' and '-OCH_3' may be beneficial to the activity. 3D-QSAR contour maps of the active compounds also suggested that increasing the volume of the side chain at position 2 of the thiazole ring may increase the activities of the TSTs [18]. Based on the above SAR, compound **3** was designed and synthesized, which was transformed from compound **2**. The activity of **3** against HIV-1 RT increased, and thus, **3** was used as the lead compound in this study. The 2,3-dihydrobenzofuran-5-yl-methylamino on the side chain at position 2 of the thiazole ring was retained, and the substituents at positions 4 and 5 of the thiazole ring were further optimized.

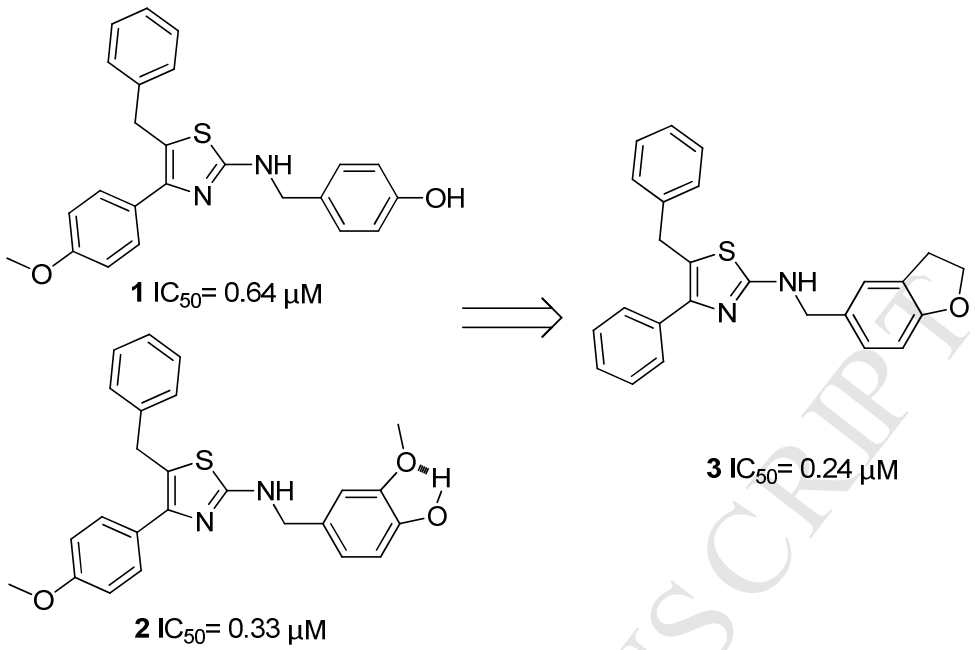

Figure 1. Structures and anti-HIV activities of compounds **1**, **2**, and **3**.

Results and discussion

The main synthetic route for the target compounds, which is described in reference 15, is shown in Scheme 1. Appropriate benzaldehydes and acetophenones were condensed to provide chalcones, which were then hydrogenated, brominated, and condensed with an appropriate sulfur source to afford 2-aminothiazoles. The 2-aminothiazoles were condensed with appropriate benzaldehydes to afford the Schiff bases. Reduction of the Schiff bases afforded the target compounds.

Scheme 1. Synthesis of **3-23**.

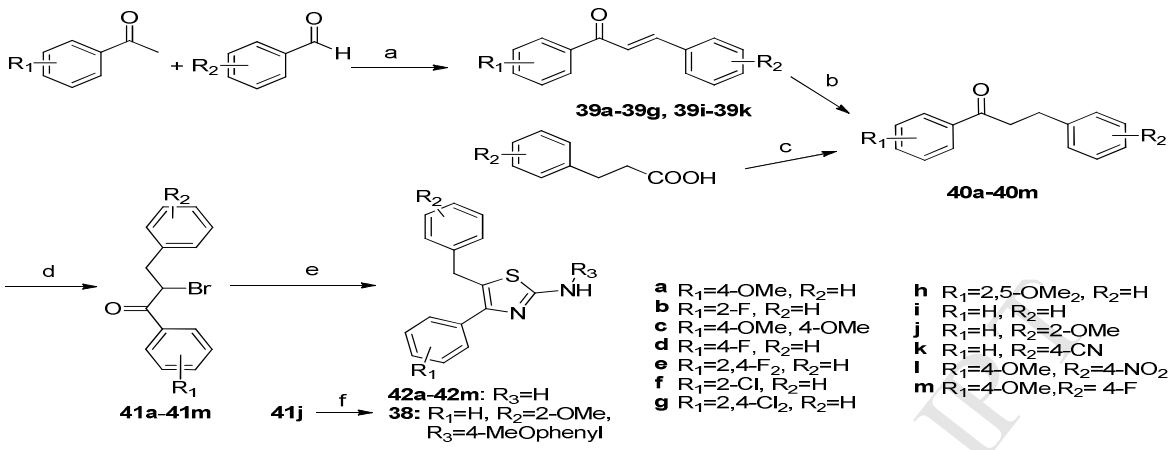

Reagents and conditions: (a) 10% NaOH, EtOH, rt, 5-10 h, 70-90% yield; (b) H_2, Pd/C, EA, rt, 3-4 h, 80-95% yield; (d) Br_2, $AlCl_3$, $CHCl_3$, 0°C, 5-10 h; (e) thiourea, CH_3COONa, EtOH, 80°C, 10-15 h, 70-80% yield; (f) 2,3-dihydrobenzofuran-5-carbaldehyde, *p*-toluenesulfonic acid, toluene, 130°C, 10-24 h, 29-80% yield.

The structures of compounds **3-23** and their activities against wild-type HIV are shown in Table 1. According to our previous study [18], we first retained the benzene ring as the substituent at position 4 of the thiazole ring and changed the substituents at position 5. Comparing compound **3** with compounds **4**, **5** and **6**, the activity substantially increased when "-OCH_3" was introduced at the ortho position of the phenyl ring at position 5, slightly increased when introduced at the meta position and almost disappeared when introduced at the para position, thus suggesting that the ortho position is the optimal position for substitution. The IC_{50} values of compounds **7** and **8** also supported this deduction. The activities of these compounds revealed that the introduction of an electron-donating group, '-OCH_3', on the ortho position of the benzene ring at position 5 of the thiazole scaffold may be beneficial. Then, considering the extensively used strategy to introduce halogen atoms and perform multi-substitutions in a drug structure to yield enhanced activity, compounds **9** and **10** were synthesized and exhibited potent IC_{50} values, suggesting that disubstitution on the benzene ring at this position led to a marked increase in activity.

In our previous study, compounds with the substituents “2-F”, “2-Cl”, “2,4-F_2” and “2,4-Cl_2” on position 4 showed potent inhibitory activities. However, only four compounds with the above-mentioned substituents were obtained in the previous study, and all exhibited good activity, a finding that indicated tremendous potential for higher activity, but further investigation was needed to confirm the effect of certain substituents. According to the results described above, we selected ‘2-OCH_3’, ‘2,6-Cl_2’, and ‘3,5-F_2’ as the optimal substituents on the benzene ring at position 5 to explore the influence of the mentioned substituents at position 4.

As shown in Table 1, the comparisons of compound **11** with compound **17** and compound **13** with compound **19** revealed that most compounds with a 2-F-phenyl at position 4 exhibited higher activities than the corresponding compounds with a 2,4-F_2-phenyl at the same position. Furthermore, the IC_{50} values of compounds **14** to **16,** which have a “-Cl” at the ortho position, and of compounds **20** to **22,** which have a 2,4-Cl_2, also exhibited the same phenomenon. Additionally, the activity of compound **23** (IC_{50}=7.32 μM), which was disubstituted at the meta position, decreased more than 100-fold compared with that of compound **17** (IC_{50}=0.01 μM). These results suggested that when position 5 was occupied by the same substituent, the inhibitory activities may be primarily provided by the ortho substituent at position 4 and that the atom located on the meta position may have some negative contribution to the activity. Moreover, compounds **9** to **22** showed obviously increased activities (0.088 to 0.010 μM) compared with the lead compound **3** (0.239 μM) and the previous best compound (compound **24** in ref. 15, 0.046 μM). This finding not only demonstrates that the strategy used successfully yielded enhanced activity by the combination of the optimal substituents on positions 4 and 5 but also provides strong evidence supporting the hypothesis that increasing the bulk of the side chain at position 2 of the thiazole ring is beneficial to the activity of the TSTs. The best compounds **14**, **16**, **17**, and **19 (**0.010 μM) highlight the significance of

this investigation, which represents a successful optimization of a reasonable drug design.

Table 1. Chemical structures and cell-based antiviral activities of compounds **3-23**[a] against wild-type HIV-1

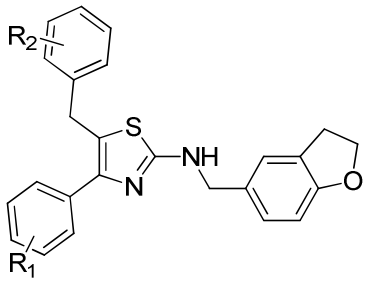

Compd	R_1	R_2	IC_{50}[b](μM)
3	H	H	0.239
4	H	2-OCH_3	0.072
5	H	3-OCH_3	0.136
6	H	4-OCH_3	>10
7	H	4-F	5.670
8	H	4-Cl	>10
9	H	2,6-Cl_2	0.062
10	H	3,5-F_2	0.037
11	2,4-F_2	2-OCH_3	0.045
12	2,4-F_2	2,6-Cl_2	0.021
13	2,4-F_2	3,5-F_2	0.014
14	2-Cl	2-OCH_3	0.010

15	2-Cl	2,6-Cl_2	0.022
16	2-Cl	3,5-F_2	0.010
17	2-F	2-OCH_3	0.010
18	2-F	2,6-Cl_2	0.032
19	2-F	3,5-F_2	0.010
20	2,4-Cl_2	2-OCH_3	0.088
21	2,4-Cl_2	2,6-Cl_2	0.071
22	2,4-Cl_2	3,5-F_2	0.068
23	3,5-F_2	2-OCH_3	7.320

[a] All tested compounds had no cytotoxicity at a final concentration of 10 μM.

[b] Inhibitory concentration 50% (IC_{50}, μM) was calculated from the dose-infectivity curves.

In our previous study, we have proved that the 2,4,5-trisubstituted thiazole derivatives' inhibitory activity on HIV-1 replication is due to the reverse transcription blockage by Time-of-Addition (TOA) assay results [18]. In this paper, we tested the four most potent compounds on reverse transcriptase activity by RT enzyme-based assay. As shown in table 2, compounds **14**, **16**, **17** and **19** inhibited RT RNA-dependent DNA polymerase activities with IC_{50} values from 0.014 to 0.064 μM; and NVP, a NNRTI targeting RNA-dependent DNA polymerase, was used as positive control with IC_{50} as 2.1 μM. This indicated that the primary target of 2,4,5-trisubstituted thiazole derivatives for their anti-HIV activities is RT RNA-dependent DNA polymerase, i.e., they are NNRTIs.

Table 2. Antiviral activities of compound 14, 16, 17 and 19 against wild-type HIV-1

Compd	IC_{50} (μM)	
	RNA-dependent DNA polymerase [a]	VSVG/HIV-1 [b]
14	0.014 ± 0.0028	0.01
16	0.025 ± 0.0057	0.01
17	0.020 ± 0.0085	0.01
19	0.064 ± 0.00071	0.01
NVP	2.1 ± 0.087	0.031

[a.] Enzyme-based antiviral assay (Average ± SD, n = 2)

[b.] Cell-based antiviral assay

[c.] NVP: Nevirapine

Resistance

Potent activity against resistant HIV-1 is an important feature for the discovery of novel NNRTIs. Therefore, six compounds, **4**, **9**, **10**, **11**, **13**, **and 16,** were selected for evaluation of their activities against NNRTI-resistant HIV-1 replication. Nine NNRTI-resistant HIV-1 recombinant virus models were used: $HIV_{RT\text{-}Y181C}$, $HIV_{RT\text{-}K103N}$, $HIV_{RT\text{-}L100I/RT\text{-}K103N}$, $HIV_{RT\text{-}Y188L}$, $HIV_{RT\text{-}K103N/RT\text{-}P225H}$, $HIV_{RT\text{-}K103N/RT\text{-}G190A}$ and $HIV_{RT\text{-}K103N/RT\text{-}V108I}$, $HIV_{RT\text{-}K103N,Y181C}$ and $HIV_{RT\text{-}K103N,Y188L}$. Compound **11** exhibited high activity against seven of the nine resistant strains, with IC_{50} values ranging from 2.9- to 23.5-fold greater than the values against wild-type HIV, which is better than that of the positive control drugs nevirapine (90- to 2152-fold) and efavirenz (5.4- to 2394-fold). However, when the viruses carried a mutation at RT-Try188, such as $HIV_{RT\text{-}Y188L}$ or $HIV_{RT\text{-}K103N/Y188L}$, the viruses exhibited severe resistance to this series of compounds (Table

3). The docking result showed that the Y188 residue may have a π-π stacking interaction with the phenyl ring at the 5 position of the thiazole. We hypothesize that this interaction plays a key role in the mutual effect between the compounds and the enzyme.

Table 3. Inhibitory effects of **4**, **9**, **10**, **11**, **13**, **16** and the references NVP and EFV on wild-type and NNRTI-resistant HIV-1 replication, as determined through a cell-based antiviral assay

Compd / Resistance	**4** IC_{50} (μM)	**9** IC_{50} (μM)	**10** IC_{50} (μM)	**11** IC_{50} (μM)	**13** IC_{50} (μM)	**16** IC_{50} (μM)	**NVP** IC_{50} (μM)	**EFV** IC_{50} (μM)
VSVG/HIV_{wt}[a]	0.072	0.0618	0.0372	0.0447	0.0139	0.010	0.031	0.00104
VSVG/HIV_{RT-} K103N	0.88 (12.2)*	1.53 (24.8)	1.41 (37.9)	0.29 (6.5)	0.2 (14)	0.08 (7.8)	16.1 (519)	0.0588 (56)
VSVG/HIV_{RT-} Y181C	0.512 (8.8)	0.39 (6.3)	5.56 (149.5)	0.13 (2.9)	1.1 (79)	0.4 (39)	66.7 (2152)	0.00565 (5.4)
VSVG/HIV_{RT-} L100I,K103N	5.31 (73.8)	5.05 (81.7)	1.17 (31.5)	0.87 (19.5)	NT[b]	NT	5.0 (161)	2.49 (2394)
VSVG/HIV_{RT-} Y188L	>10 (>223.7)	>10 (>161.8)	>10 (>268.8)	>10 (>223.7)	7 (504)	1.4 (136)	>10 (>322)	0.48 (461.5)

VSVG/HIV$_{RT}$-K103N,P225H	4.98 (69.2)	>10 (>161.8)	5.03 (135.2)	1.05 (23.5)	NT	NT	5.48 (177)	0.16 (154)
VSVG/HIV$_{RT}$-K103N,G190A	0.58 (8.1)	0.56 (9.1)	2 (53.8)	0.49 (11.0)	NT	NT	>10 (>322)	0.056 (538)
VSVG/HIV$_{RT}$-K103N,V108I	1.53 (21.3)	3.0 (48.5)	10.4 (279.6)	0.76 (17.0)	3.9 (218)	0.3 (29)	2.8 (90)	0.083 (79.8)
VSVG/HIV$_{RT}$-K103N,Y181C	9.56 (132.8)	>10 (>161.8)	>10 (>268.8)	0.45 (10.1)	NT	NT	>10 (>322)	0.0587 (56.4)
VSVG/HIV$_{RT}$-K103N,Y188L	>10 (>223.7)	>10 (>161.8)	>10 (>268.8)	>10 (>223.7)	NT	NT	>10 (>322)	13.8 (13269.2)

[a.] VSV-G: vesicular stomatitis virus G protein

[b.] NT: not tested

* Mean change (fold) in IC_{50} compared to wild type.

Docking studying

Compounds **16**, **17** and **19**, which exhibited the highest activity against the WT HIV-1, were used as representatives to conduct the docking experiments in the WT HIV-1 RT non-nucleoside binding site (NNBS) and to study the binding mode of the TSTs. To take the flexibility of the experimental NNBS into account, the structural data of six RTs (1c1b, 1c1c, 1ikx, 2b5j, 3lak, and 2rki) were selected. The Surflex program was used to dock the compounds into all six RTs. The results indicated that the three compounds almost aligned in all cases, and a nearly identical binding mode for the three compounds with all RTs was

observed: (i) the two nitrogen atoms on the thiazole ring and on the side chain of position 2 formed two hydrogen bonds with the K103 and K101 amino groups, respectively; (ii) the side chain at the 2 position of the thiazole occupied a pocket formed primarily by the side chains of F227, L234, H235, P225, P226 and P236 and fit in the pocket well, which may explain why the compounds with the 2,3-dihydrobenzofuran on the side chain exhibited higher activities than the corresponding compounds with 4-methoxyphenyl on the side chain; and (iii) the phenyl ring at the 5 position of the thiazole has a π-π stacking interaction with Y181 or Y188. These possible reactions may explain the decrease in the IC_{50} of the above six compounds, **4**, **9**, **10**, **11**, **13** and **16,** against Y188 mutants. Moreover, to explain the improved activity of **11** against other mutants, we can speculate that both 2-OCH_3 on position 5 and 2,4-F_2 on position 4 may exhibit good interactions with the surrounding residues, a speculation that might require additional investigation to provide deeper insights.

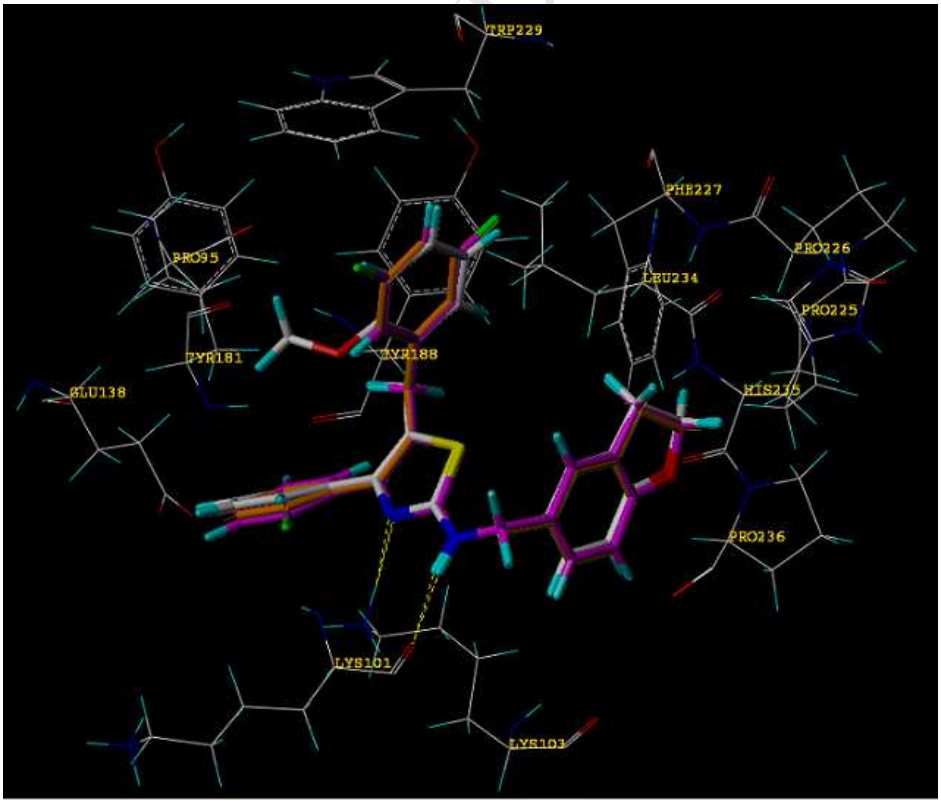

Figure 2. Binding conformation of **16** (magenta), **17** (white) and **19** (orange) into the NNBS of HIV-1WT RT (PDB id:2rki). Hydrogen bonds are shown as dotted yellow lines.

Conclusion

Based on a previous study, 21 novel 2,4,5-trisubstituted thiazole derivatives (**3-23**) were designed and synthesized. Their anti-HIV activity and the SAR analysis provided us with a deeper understanding of the mechanism of the TSTs. Among the synthesized derivatives, 19 compounds exhibited potent inhibition of HIV-1 replication with submicromolar IC_{50} values against wild-type strains. Compounds, **4**, **9**, **10**, **11**, **13** and **16** were also evaluated for their activities against nine HIV-1 RT mutants, and compound **11** exhibited high activity against seven of the nine resistant strains. RT enzymatic assay results illustrated that 2,4,5-trisubstituted thiazole derivatives are RT RNA-dependent DNA polymerase inhibitors. The docking study revealed the most likely mechanism of interaction between this type of compound and the HIV-1 RT, and the result suggested a possible steady conformation of the binding mode.

Experimental

Chemistry. The starting materials and other reagents were purchased from commercial suppliers and were used as received without further purification unless otherwise indicated. The melting points were measured using a WRS-1B digital melting point apparatus from Shanghai Measuring Instruments Equipment Co., Ltd. ^{1}H NMR and ^{13}C NMR spectra were measured on a VARIAN Mercury 600 MHz spectrometer using TMS as an internal standard. ^{1}H NMR and ^{13}C NMR spectra were obtained in DMSO-d_6 or $CDCl_3$ solutions as indicated (reported in ppm). The mass spectra were obtained using liquid chromatography mass spectrometry (LC-MS) on a Bruker APEXIIFT-ICR mass spectrometer with an ESI interface. Thin-layer chromatography (TLC) was performed using silica gel GF254. The hydrogenation reactions were conducted using a GCD-500 high-purity hydrogen generator and a BLT-2000

medium-pressure hydrogenation apparatus produced by Beijing Jiaweikechuang Company. The boiling range for petroleum ether is 60-90°C.

General procedure for the preparation of derivatives of 3-23. The 4,5-disubstituted thiazol-2-amine obtained from the previous step, a substituted aryl aldehyde (1 equivalent) and a catalytic amount of *p*-toluenesulfonic acid were added to a 50 mL round-bottom flask, and the mixture was refluxed in toluene for 24 h. Then, the solvent was removed, and sodium borohydride (5 equivalents) in ethanol was added. The mixture was stirred for 2-3 h and monitored by TLC. After the solvent was removed and the mixture was extracted, washed and concentrated, column chromatography was performed for further purification.

5-Benzyl-N-((2,3-dihydrobenzofuran-5-yl)methyl)-4-phenylthiazol-2-amine ***(3)*** was obtained as a slight yellow solid in 76.0% yield. ^{1}H NMR (DMSO-d_6, 600 MHz) δ 3.12 (t, J = 8.4 Hz, 2H, CH_2), 4.05 (s, 2H, CH_2), 4.30 (d, J = 5.4 Hz, 2H, CH_2), 4.47 (t, J = 8.4 Hz, 2H, CH_2), 6.68 (d, J = 8.4 Hz, 1H, ArH), 7.05 (d, J = 8.4 Hz, 1H, ArH), 7.19 (dd, J = 17.4, 6.6 Hz, 4H, ArH), 7.29 (t, J = 7.2 Hz, 3H, ArH), 7.38 (t, J = 7.8 Hz, 2H, ArH), 7.57-7.52 (m, 2H, ArH), 7.84 (t, J = 6.0 Hz, 1H, NH); ^{13}C NMR (151 MHz, $CDCl_3$) δ 159.70, 140.54, 135.26, 129.70, 128.52, 128.25, 127.70, 127.51, 126.49, 124.54, 109.17, 77.21, 77.00, 76.79, 71.33, 49.59, 32.93, 29.64; ESI-MS *m/z*: 477 ($[M + H]^+$; m.p. 125.3-126.4°C.

N-((2,3-Dihydrobenzofuran-5-yl)methyl)-5-(2-methoxybenzyl)-4-phenylthiazol-2-amine ***(4)*** was obtained as a white solid in 55.1% yield. ^{1}H NMR (DMSO-d_6, 600 MHz) δ 3.14 (t, J= 8.4 Hz, 2H, CH_2CH_2), 3.75 (s, 3H, OCH_3), 3.98 (s, 2H, $ArCH_2$), 4.31 (d, J= 6.0 Hz, 2H, $ArCH_2N$), 4.49 (t, J= 8.4 Hz, 2H, CH_2CH_2), 6.70 (d, J= 7.8 Hz, 1H, ArH), 6.88 (t, J= 7.2 Hz, 1H, ArH), 6.98 (d, J= 8.4 Hz, 1H, ArH), 7.07 (d, J= 7.2 Hz, 2H, ArH), 7.22 (m, 2H, ArH), 7.30 (t, J= 7.2 Hz, 1H, ArH), 7.39 (t, J= 7.2 Hz, 2H, ArH), 7.56 (d, J= 7.2 Hz, 2H, ArH), 7.80 (t, J= 6.0 Hz, 1H, NH); ^{13}C NMR (151 MHz, $CDCl_3$) δ 166.91, 159.64, 156.99, 147.40, 135.61, 129.91, 129.36, 128.95, 128.50, 128.21, 127.70, 127.43, 127.29, 124.54,

120.54, 119.76, 110.13, 109.11, 77.24, 77.02, 76.81, 71.33, 55.17, 49.56, 29.66, 27.25; IR (KBr, cm^{-1}): 3206(ν_{N-H}), 3098, 2966, 2891, 1582, 1491, 1461, 1430, 1331, 1244, 1167, 1103, 975, 818, 755, 700; ESI-HRMS: Calcd. for $C_{26}H_{24}N_2O_2S$: *m/z* 429.1637 $[M + H]^+$, found: 429.1597; m.p. 128.5-129.5°C.

N-((2,3-Dihydrobenzofuran-5-yl)methyl)-5-(3-methoxybenzyl)-4-phenylthiazol-2-amine ***(5)*** was obtained as slight yellow solid in 75.0% yield. ^{1}H NMR (DMSO-d_6, 600 MHz) δ 3.12 (t, J = 8.4 Hz, 2H, CH_2), 3.68 (s, 3H, OCH_3), 4.05 (s, 2H, CH_2), 4.33-4.28 (d, J = 5.4 Hz, 2H, CH_2), 4.47 (t, J = 8.4 Hz, 2H, CH_2), 6.68 (d, J = 8.4 Hz, 1H, ArH), 6.84-6.69 (m, 3H, ArH), 7.05 (d, J = 8.4 Hz, 1H, ArH), 7.22-7.19 (m, 1H, ArH), 7.29 (dd, J = 8.4, 6.6 Hz, 1H, ArH), 7.38 (td, J = 7.8, 2.4 Hz, 2H, ArH), 7.60-7.42 (m, 3H, ArH), 7.85 (t, J = 5.4 Hz, 1H, NH); ^{13}C NMR (151 MHz, $CDCl_3$) δ 159.74, 159.16, 142.16, 140.76, 135.27, 133.21, 129.82, 128.37, 127.62, 124.53, 120.56, 115.92, 114.50, 113.98, 113.62, 111.80, 109.16, 77.22, 77.01, 76.80, 71.34, 55.41, 55.17, 49.57, 33.53, 32.91, 29.64; ESI-MS *m/z*: 429 [M + H]+; m.p. 115.8-117.5°C.

N-((2,3-Dihydrobenzofuran-5-yl)methyl)-5-(4-methoxybenzyl)-4-phenylthiazol-2-amine ***(6)*** was obtained as a slight yellow solid in 45.5% yield. ^{1}H NMR (DMSO-d_6, 600 MHz) δ 3.70 (s, 3H, OCH_3), 3.73 (s, 3H, OCH_3), 4.02 (s, 2H, CH_2), 4.36 (d, J=6.0 Hz, 2H, CH_2), 6.76-6.79 (m, 1H, ArH), 6.89-6.93 (m, 4H, ArH), 7.17-7.21 (m, 4H, ArH), 7.27 (t, J=7.2, 2H, ArH), 7.44-7.47 (m, 2H, ArH), 7.89 (t, J=6.0 Hz, 1H, NH); ^{13}C NMR (151 MHz, $CDCl_3$) δ 167.61, 159.81, 159.03, 146.91, 140.57, 139.56, 129.62, 128.56, 128.17, 127.69, 126.67, 129.56, 119.67, 118.43, 113.71, 113.07, 112.76, 55.22, 55.18, 49.66, 32.88; ESI-MS *m/z* 417 $[M + H]^+$.

N-((2,3-Dihydrobenzofuran-5-yl)methyl)-5-(4-fluorobenzyl)-4-phenylthiazol-2-amine ***(7)*** was obtained as a white solid in 42% yield. ^{1}H NMR (600 MHz, DMSO-d_6) δ 3.14 (t, J = 8.7 Hz, 2H, CH_2), 4.07 (s, 2H,

CH_2), 4.36-4.29 (m, 2H, CH_2), 4.49 (td, *J* = 8.7, 1.7 Hz, 2H, CH_2), 6.70 (dd, *J* = 8.2, 1.6 Hz, 1H, ArH), 7.07 (d, *J* = 8.2 Hz, 1H, ArH), 7.12 (td, *J* = 8.7, 1.7 Hz, 2H, ArH), 7.24-7.19 (m, 3H, ArH), 7.33-7.28 (m, 1H, ArH), 7.40 (td, *J* = 7.7, 1.7 Hz, 2H, ArH), 7.58-7.53 (m, 2H, ArH), 7.90-7.85 (t, *J* = 5.4 Hz, 1H, NH_2); ^{13}C NMR (151 MHz, $CDCl_3$) δ 167.10, 162.41, 160.79, 159.71, 147.09, 136.09, 134.88, 129.70, 128.41, 127.68, 127.50, 124.51, 119.56, 115.44, 115.30, 109.16, 77.23, 77.01, 76.80, 71.34, 49.59, 32.13, 29.64; IR(KBr, cm^{-1}): 3309, 1552, 1508, 1490, 1352, 1223, 1104, 831, 694; m.p. 153-154.5°C.

5-(4-Chlorobenzyl)-N-((2,3-dihydrobenzofuran-5-yl)methyl)-4-phenylthiazol-2-amine ***(8)*** was obtained as a slight yellow solid in 76.0% yield. ^1H NMR (DMSO-d_6, 600 MHz) δ 3.14 (t, *J* = 8.4 Hz, 2H, CH_2), 4.07 (s, 2H, CH_2), 4.33 (dd, *J* = 15.6, 5.4 Hz, 2H, CH_2), 4.49 (t, *J* = 8.4 Hz, 2H, CH_2), 6.70 (d, *J* = 8.4 Hz, 1H, ArH), 7.07 (d, *J* = 8.4 Hz, 1H, ArH), 7.24-7.18 (m, 3H, ArH), 7.33-7.28 (m, 1H, ArH), 7.42-7.33 (m, 4H, ArH), 7.54 (d, *J* = 8.4 Hz, 2H, ArH), 7.90 (t, *J* = 5.4 Hz, 1H, NH); ^{13}C NMR (151 MHz, $CDCl_3$) δ 167.12, 159.69, 147.81, 139.01, 135.15, 132.27, 129.58, 128.68, 128.39, 127.64, 127.48, 124.48, 119.07, 109.16, 77.23, 77.01, 76.80, 71.33, 49.55, 32.28, 29.65; ESI-MS *m/z*: 433 $[M + H]^+$; m.p. 137.2-137.8°C.

5-(2,6-Dichlorobenzyl)-N-((2,3-dihydrobenzofuran-5-yl)methyl)-4-phenylthiazol-2-amine ***(9)*** was obtained as a slight yellow in 76.0% yield. ^1H NMR (DMSO-d_6, 600 MHz) δ 3.13 (t, *J* = 8.4 Hz, 2H, CH_2), 4.29 (d, *J* = 5.4 Hz, 2H, CH_2), 4.36 (s, 2H, CH_2), 4.48 (t, *J* = 8.4 Hz, 2H, CH_2), 6.68 (d, *J* = 7.8 Hz, 1H, ArH), 7.04 (d, *J* = 7.8 Hz, 1H, ArH), 7.19 (s, 1H, ArH), 7.30 (t, *J* = 7.8 Hz, 1H, ArH), 7.34 (t, *J* = 7.8 Hz, 1H, ArH), 7.44 (t, *J* = 6.6 Hz, 4H, ArH), 7.64 (d, *J* = 7.8 Hz, 2H, ArH), 7.76 (t, *J* = 5.4 Hz, 1H, NH); ^{13}C NMR (151 MHz, $CDCl_3$) δ 166.62, 159.66, 147.66, 136.59, 135.73, 135.54, 129.74, 128.70, 128.45, 128.25, 127.70, 127.43, 124.55, 117.61, 109.14, 77.22, 77.01, 76.80, 71.32, 49.61, 29.63, 29.30; ESI-MS *m/z*: 467 $[M + H]^+$; m.p. 147.2-148.9°C.

5-(3,5-Difluorobenzyl)-N-((2,3-dihydrobenzofuran-5-yl)methyl)-4-phenylthiazol-2-amine ***(10)*** was obtained as a slight yellow solid in 79% yield. mp:158.4-159.5℃, ^{1}H NMR (DMSO-d_6, 600 MHz) δ 3.15 (t, J = 8.4 Hz, 2H, -O-CH2-CH2-), 4.11 (s, 2H, CH2), 4.34 (dd, J = 15.6, 6.0 Hz, 2H, -NH-CH2-), 4.49 (t, J = 8.4 Hz, 2H, -O-CH2-CH2-), 6.70 (d, J = 8.4 Hz, 1H, ArH), 6.88 (d, J = 6.6 Hz, 2H, ArH), 7.09 (t, J = 9.0 Hz, 2H, ArH), 7.24 (d, J = 11.4 Hz, 1H, ArH), 7.32 (t, J = 7.2 Hz, 1H, ArH), 7.40 (t, J = 7.8 Hz, 2H, ArH), 7.53 (d, J = 7.2 Hz, 2H, ArH), 7.94 (t, J = 5.4 Hz, 1H, -NH-CH2-); ^{13}C NMR (151 MHz, $CDCl_3$) δ 167.37, 163.95, 162.30, 159.71, 148.52, 144.55, 134.99, 129.57, 128.40, 127.71, 127.50, 124.46, 117.44, 110.99, 109.17, 102.18, 102.01, 101.84, 77.23, 77.01, 76.80, 71.34, 49.53, 32.52, 29.64; ESI-MS *m/z*: 435 [M + H]+.

4-(2,4-Difluorophenyl)-N-((2,3-dihydrobenzofuran-5-yl)methyl)-5-(2-methoxybenzyl)thiazol-2-amine ***(11)*** was obtained as a slight yellow solid in 72% yield. ^{1}H NMR(DMSO-d_6, 600 MHz) δ 3.13 (t, J = 8.4 Hz, 2H, -O-CH_2-CH_2-), 3.66 (d, J = 8.4 Hz, 3H, OCH_3), 3.72 (s, 2H, CH_2), 4.26 (d, J = 5.4 Hz, 2H, -NH-CH_2-), 4.48 (t, J = 8.4 Hz, 2H, -O-CH_2-CH_2-), 6.67 (d, J = 8.4 Hz, 1H, ArH), 6.83 (t, J = 7.2 Hz, 1H, ArH), 6.91 (d, J = 8.4 Hz, 1H, ArH), 6.98 (d, J = 7.2 Hz, 1H, ArH), 7.03 (d, J = 8.4 Hz, 1H, ArH), 7.23-7.10 (m, 3H, ArH), 7.30 (t, J = 9.6 Hz, 1H, ArH), 7.47 (dd, J = 15.6, 7.2 Hz, 1H, ArH), 7.81 (t, J = 5.4 Hz, 1H, -NH-CH_2-); ^{13}C NMR (151 MHz, $CDCl_3$) δ 167.32, 163.40, 161.75, 160.93, 159.70, 159.27, 156.89, 140.35, 132.61, 129.71, 128.59, 127.82, 127.67, 127.50, 124.51, 122.89, 111.14, 110.18, 109.14, 104.28, 104.11, 103.94, 77.22, 77.01, 76.80, 71.34, 55.09, 49.55, 29.63, 27.19; ESI-MS *m/z*: 465 $[M + H]^+$; m.p. 126.8-127.7°C.

5-(2,6-Dichlorobenzyl)-4-(2,4-difluorophenyl)-N-((2,3-dihydrobenzofuran-5-yl)methyl)thiazol-2-amine ***(12)*** was obtained as a slight yellow solid in 70.0% yield. ^{1}H NMR(DMSO-d_6, 600 MHz) δ 3.19-3.07 (m, 2H, -O-CH_2-CH_2-), 4.07 (s, 2H, CH_2), 4.26 (d, J = 5.4 Hz, 2H, -NH-CH_2-), 4.53-4.45 (m, 2H,

-O-CH_2-CH_2-), 6.68 (d, *J* = 8.4 Hz, 1H, ArH), 7.03 (t, *J* = 9.6 Hz, 1H, ArH), 7.16 (dd, *J* = 22.2, 13.8 Hz, 2H, ArH), 7.28 (t, *J* = 8.4 Hz, 1H, ArH), 7.34 (t, *J* = 9.6 Hz, 1H, ArH), 7.43 (d, *J* = 8.4 Hz, 2H, ArH), 7.55 (dd, *J* = 15.6, 7.8 Hz, 1H, ArH), 7.85 (t, *J* =5.4 Hz, 1H, -NH-CH_2-); ^{13}C NMR (151 MHz, $CDCl_3$) δ 167.08, 161.80, 159.77, 141.00, 136.18, 135.44, 132.63, 129.47, 128.48, 128.33, 128.02, 127.73, 127.55, 124.58, 120.06, 111.38, 109.22, 104.27, 104.10, 103.93, 77.23, 77.01, 76.80, 71.36, 49.63, 29.63, 29.06; ESI-MS *m/z*: 503 $[M + H]^+$; m.p. 143.8-145.1°C.

5-(3,5-Difluorobenzyl)-4-(2,4-difluorophenyl)-N-((2,3-dihydrobenzofuran-5-yl)methyl)thiazol-2-amine ***(13)*** was obtained as a slight yellow solid in 76.0% yield. ^{1}H NMR(DMSO-d_6, 600 MHz) δ 3.12 (t, *J* = 8.4 Hz, 2H, -O-CH_2-CH_2-), 3.83 (s, 2H, CH_2), 4.27 (d, *J* = 5.4 Hz, 2H, -NH-CH_2-), 4.47 (t, *J* = 8.4 Hz, 2H, -O-CH_2-CH_2-), 6.68 (d, *J* = 7.8 Hz, 1H, ArH), 6.79 (d, *J* = 7.8 Hz, 2H, ArH), 7.04 (d, *J* = 7.2 Hz, 2H, ArH), 7.13 (t, *J* = 8.4 Hz, 1H, ArH), 7.19 (s, 1H, ArH), 7.30 (t, *J* = 9.6 Hz, 1H, ArH), 7.48 (dd, *J* = 15.6, 7.8 Hz, 1H, ArH), 7.95 (t, *J* = 5.4 Hz, 1H, -NH-CH_2-); ^{13}C NMR (151 MHz, $CDCl_3$) δ 167.64, 163.82, 163.57, 162.17, 161.91, 160.62, 159.79, 159.04, 143.99, 141.37, 132.55, 129.29, 127.61, 124.45, 120.83, 119.2, 111.54, 111.13, 109.23, 104.41, 104.23, 104.07, 102.21, 102.05, 101.88, 77.21, 77.00, 76.79, 71.35, 49.54, 32.62, 29.62; ESI-MS *m/z*: 471 $[M + H]^+$; m.p. 112.7-114.4°C.

4-(2-Chlorophenyl)-N-((2,3-dihydrobenzofuran-5-yl)methyl)-5-(2-methoxybenzyl)thiazol-2-amine ***(14)*** was obtained as a white solid in 55.0% yield. ^{1}H NMR(DMSO-d_6, 600 MHz) δ 3.13 (t, *J* = 8.7 Hz, 2H, CH_2), 3.66 (s, 2H, CH_2), 3.69 (d, *J* = 1.1 Hz, 3H, OCH_3), 4.26 (d, *J* = 5.6 Hz, 2H, CH_2), 4.49 (td, *J* = 8.8, 1.3 Hz, 2H, CH_2), 6.68 (d, *J* = 8.1 Hz, 1H, ArH), 6.82 (td, *J* = 7.4, 1.1 Hz, 1H, ArH), 6.91 (d, *J* = 8.2 Hz, 1H, ArH), 6.95 (dd, *J* = 7.4, 1.5 Hz, 1H, ArH), 7.05 (dd, *J* = 8.2, 1.7 Hz, 1H, ArH), 7.17 (td, *J* = 7.8, 1.6 Hz, 1H, ArH), 7.22 (s, 1H, ArH), 7.39 (m, 3H, ArH), 7.53 (m, 1H, ArH), 7.79 (s, 1H, NH); ^{13}C NMR (151 MHz, $CDCl_3$) δ 167.26, 159.60, 156.86, 144.62, 134.86, 134.22, 132.00, 129.84, 129.65, 129.18, 128.71,

127.70, 127.39, 126.40, 124.58, 122.12, 120.42, 110.12, 109.04, 71.32, 55.07, 49.50, 29.65, 27.15; IR(KBr, cm^{-1}): 3088(ν_{C-H}), 2965, 2887(ν_{C-H}), 1579, 1484(ν_{Ar}), 1327(δ_{C-H}), 1244(ν_{C-O}), 1098(ν_{C-O}), 1020, 819, 752(δ_{C-H}); ESI-MS *m/z*: 462 $[M + H]^+$; m.p. 129.4-131.1°C.

4-(2-Chlorophenyl)-5-(2,6-dichlorobenzyl)-N-((2,3-dihydrobenzofuran-5-yl)methyl)thiazol-2-amine ***(15)*** was obtained as a white solid in 34% yield. ^{1}H NMR (DMSO-d_6, 600 MHz) δ 3.12 (t, J = 8.4 Hz, 2H, CH_2), 4.02 (s, 2H, CH_2), 4.25 (d, J = 6.0 Hz, 2H, CH_2), 4.48 (t, J = 8.4 Hz, 2H, CH_2), 6.67 (d, J = 8.4 Hz, 1H, ArH), 7.05-7.01 (m, 1H, ArH), 7.20 (s, 1H, ArH), 7.27 (t, J =7.8Hz, 1H, ArH), 7.47-7.39 (m, 5H, ArH), 7.56-7.53 (m, 1H, ArH), 7.81 (t, J = 5.4 Hz, 1H, NH); ^{13}C NMR (151 MHz, $CDCl_3$) δ 166.85, 159.72, 145.17, 136.22, 135.48, 134.64, 134.03, 132.04, 129.66, 129.30, 128.34, 127.77, 127.50, 126.49, 124.65, 119.53, 109.18, 77.23, 77.02, 76.81, 71.35, 49.65, 29.65, 29.22; IR(KBr, cm^{-1}): 3422, 3200, 3093, 2931, 1587, 1560, 1492, 1434, 1249, 983, 939, 762; ESI-MS *m/z* 501$[M+1]^+$; m.p. 179-181°C.

4-(2-Chlorophenyl)-5-(3,5-difluorobenzyl)-N-((2,3-dihydrobenzofuran-5-yl)methyl)thiazol-2-amine ***(16)*** was obtained as a yellow solid in 51.3% yield. ^{1}H NMR(DMSO-d_6, 600 MHz) δ 3.14 (t, J = 8.7 Hz, 2H, CH_2), 3.79 (s, 2H, CH_2), 4.28 (d, J = 5.6 Hz, 2H, CH_2), 4.49 (t, J = 8.7 Hz, 2H, CH_2), 6.69 (d, J = 8.1 Hz, 1H, ArH), 6.77 (m, 2H, ArH), 7.09-6.99 (m, 2H, ArH), 7.23 (d, J = 1.7 Hz, 1H, ArH), 7.41 (m, J = 9.5, 7.8, 6.4, 2.0 Hz, 3H, ArH), 7.54 (dt, J = 6.7, 1.4 Hz, 1H, ArH), 7.95 (d, J = 6.4 Hz, 1H, NH); ^{13}C NMR (151 MHz, $CDCl_3$) δ 163.77, 162.13, 159.74, 144.07, 134.03, 131.77, 129.82, 129.60, 129.39, 127.73, 127.52, 126.67, 124.57, 111.13, 109.17, 102.11, 101.94, 101.77, 71.35, 49.56, 32.57, 29.63; IR(KBr, cm^{-1}): 3094(ν_{C-H}), 2943(ν_{C-H}), 1624, 1579, 1484(ν_{Ar}), 1316(ν_{C-N}), 1115(ν_{C-N}), 886, 757(δ_{C-H}); ESI-MS *m/z*: 468 $[M + H]^+$; m.p. 89.9-92.2°C.

N-((2,3-Dihydrobenzofuran-5-yl)methyl)-4-(2-fluorophenyl)-5-(2-methoxybenzyl)thiazol-2-amine ***(17)***

was obtained as a slight yellow solid in 63.0% yield. ^{1}H NMR(DMSO-d_6, 600 MHz) δ 3.12 (td, J = 8.8, 2.7 Hz, 2H), 3.65 (d, J = 9.4 Hz, 3H), 3.72 (d, J = 3.3 Hz, 2H), 4.25 (dd, J = 8.3, 5.8 Hz, 2H), 4.47 (td, J = 8.7, 1.9 Hz, 2H), 6.67 (dd, J = 8.1, 3.4 Hz, 1H), 6.81 (t, J = 7.4 Hz, 1H), 6.88 (dd, J = 14.2, 8.4 Hz, 1H), 6.95 (m, 1H), 7.05-7.01 (m, 1H), 7.08 (d, J = 2.5 Hz, 1H), 7.00-7.13 (m, 1H), 7.24 (q, J = 8.8, 7.5 Hz, 2H), 7.44-7.31 (m, 2H), 7.68 (ddt, J = 28.4, 5.9, 3.4 Hz, 1H), 7.81 (dt, J = 32.8, 5.8 Hz, 1H); ^{13}C NMR (151 MHz, $CDCl_3$) δ 167.29, 160.79, 159.71, 159.15, 156.93, 156.07, 141.38, 132.29, 131.82, 131.05, 130.33, 129.83, 128.83, 127.75, 127.51, 124.59, 123.94, 123.47, 122.87, 121.52, 120.47, 115.86, 111.84, 110.18, 109.16, 71.36, 55.39, 55.11, 49.60, 29.66, 27.22, 27.00; IR(KBr, cm^{-1}): 3188(ν_{C-H}), 2926(ν_{C-H}), 1585, 1490(ν_{Ar}), 1244(ν_{C-O}), 1115(ν_{C-O}), 1026, 819, 763(δ_{C-H}); ESI-MS *m/z*: 446 [M + H]$^{+}$; m.p. 96.1-98.0°C.

5-(2,6-Dichlorobenzyl)-N-((2,3-dihydrobenzofuran-5-yl)methyl)-4-(2-fluorophenyl)thiazol-2-amine ***(18)*** was obtained as a white solid in 41% yield. ^{1}H NMR (DMSO-d_6, 600 MHz) δ 3.13 (t, J = 8.4 Hz, 2H, CH_2), 4.09 (s, 2H, CH_2), 4.27 (d, J = 6.0 Hz, 2H, CH_2), 4.48 (t, J = 8.4 Hz, 2H), 6.68 (d, J = 8.4 Hz, 1H, ArH), 7.05 – 7.01 (m, 1H, ArH), 7.20 – 7.17 (m, 1H, ArH), 7.32 – 7.26 (m, 3H, ArH), 7.51 (td, J = 7.8, 1.8 Hz, 1H, ArH), 7.83 (t, J = 6.0 Hz, 1H, NH); IR(KBr, cm^{-1}): 3192, 3088, 2926, 1537, 1489, 1433, 1331, 1248, 1218, 980, 929, 775, 752; ESI-MS *m/z* 485 [M+H]$^{+}$; m.p. 140-141.5°C.

5-(3,5-Difluorobenzyl)-N-((2,3-dihydrobenzofuran-5-yl)methyl)-4-(2-fluorophenyl)thiazol-2-amine ***(19)*** was obtained as a white solid in 43% yield. ^{1}H NMR (600 MHz, DMSO-d6) δ 7.96 (t, J = 5.8 Hz, 1H), 7.48-7.39 (m, 2H), 7.30-7.23 (m, 2H), 7.22 (s, 1H), 7.09-7.02 (m, 2H), 6.81 (h, J = 4.6 Hz, 2H), 6.70 (d, J = 8.0 Hz, 1H), 4.49 (t, J = 8.7 Hz, 2H), 4.30 (d, J = 5.7 Hz, 2H), 3.86 (s, 2H), 3.14 (t, J = 8.7 Hz, 2H); ^{13}C NMR (151 MHz, $CDCl_3$) δ 167.70, 163.82, 162.18, 160.54, 159.79, 158.90, 144.24, 131.73, 129.92, 129.38, 127.71, 127.56, 124.52, 124.22, 122.84, 120.74, 116.05, 115.90, 111.19, 109.22, 102.16, 101.99, 101.82, 77.23, 77.02, 76.81, 71.37, 49.59, 32.73, 29.65; IR(KBr, cm$_{-1}$): 3201, 3096, 2931, 1590, 1492,

1459, 1326, 1114, 987, 764; m.p. 104.5-106°C.

4-(2,4-Dichlorophenyl)-N-((2,3-dihydrobenzofuran-5-yl)methyl)-5-(2-methoxybenzyl)thiazol-2-amine ***(20)*** was obtained as a white solid in 80.0% yield. ^{1}H NMR (DMSO-d_6, 600 MHz) δ 3.11 (t, J = 8.4 Hz, 2H, -O-CH_2-CH_2-), 3.64 (s, 2H, CH_2), 3.67 (s, 3H, OCH_3), 4.23 (d, J = 5.4 Hz, 2H, -NH-CH_2-), 4.46 (t, J = 8.4 Hz, 2H, -O-CH_2-CH_2-), 6.66 (d, J = 8.4 Hz, 1H, ArH), 6.81 (t, J = 7.8 Hz, 1H, ArH), 6.89 (d, J = 8.4 Hz, 1H, ArH), 6.97 – 6.93 (m, 1H, ArH), 7.02 (d, J = 8.4 Hz, 1H, ArH), 7.18 – 7.13 (m, 1H, ArH), 7.19 (s, 1H, ArH), 7.38 (d, J = 8.4 Hz, 1H, ArH), 7.46 (dd, J = 8.4, 2.4 Hz, 1H, ArH), 7.67 (d, J = 2.4 Hz, 1H, ArH), 7.80 (t, J = 5.4 Hz, 1H, -NH-CH_2-); ^{13}C NMR (151 MHz, $CDCl_3$) δ 167.19, 159.67, 156.83, 143.48, 135.01, 134.28, 133.46, 132.73, 129.57, 128.44, 127.82, 127.56, 126.74, 124.52, 122.73, 120.44, 110.15, 109.11, 77.22, 77.01, 76.80, 71.33, 55.06, 49.53, 29.65, 27.20; ESI-MS *m/z*: 497 $[M + H]^+$; m.p. 147.7-148.5°C.

5-(2,6-Dichlorobenzyl)-4-(2,4-dichlorophenyl)-N-((2,3-dihydrobenzofuran-5-yl)methyl)thiazol-2-amine ***(21)*** was obtained as a white solid in 29% yield. ^{1}H NMR (DMSO-d_6, 600 MHz) δ 3.12 (t, J = 8.7 Hz, 2H, CH_2), 4.02 (s, 2H, CH_2), 4.25 (d, J = 5.7 Hz, 2H, CH_2), 4.48 (t, J = 8.7 Hz, 2H, CH_2), 6.67 (d, J = 8.1 Hz, 1H, ArH), 7.02 (dd, J = 8.1, 1.8 Hz, 1H, ArH), 7.19 (d, J = 1.8 Hz, 1H, ArH), 7.28 (dd, J = 8.4, 7.7 Hz, 1H, ArH), 7.43 (d, J = 8.0 Hz, 2H, ArH), 7.51-7.45 (m, 2H, ArH), 7.71 (d, J = 1.9 Hz, 1H, ArH), 7.86 (t, J = 5.7 Hz, 1H, NH); ^{13}C NMR (151 MHz, $CDCl_3$) δ *1*66.86, 135.41, 132.78, 129.88, 129.52, 129.34, 128.50, 128.33, 127.79, 127.56, 126.89, 124.65, 120.02, 109.22, 77.20, 76.99, 76.78, 71.35, 49.66, 29.76, 29.70, 29.37; IR(KBr, cm^{-1}): 2980, 2927, 1474, 1253, 1056, 1026, 966, 848; ESI-MS *m/z:* 536 $[M+3]^+$; m.p. 172.5-173.5°C.

4-(2,4-Dichlorophenyl)-5-(3,5-difluorobenzyl)-N-((2,3-dihydrobenzofuran-5-yl)methyl)thiazol-2-amine

(22) was obtained as a yellow solid in 53.6% yield. ^{1}H NMR (600 MHz, DMSO-d_6) δ 7.97 (t, J = 5.7 Hz, 1H, ArH), 7.70 (d, J = 2.1 Hz, 1H, ArH), 7.47 (dd, J = 8.3, 2.1 Hz, 1H, ArH), 7.43 (d, J = 8.3 Hz, 1H, ArH), 7.25-7.20 (m, 1H, ArH), 7.08-7.00 (m, 2H, ArH), 6.78 (h, J = 4.4 Hz, 2H, ArH), 6.69 (d, J = 8.1 Hz, 1H,NH), 4.49 (t, J = 8.7 Hz, 2H,OCH_2CH_2), 4.28 (d, J = 5.7 Hz, 2H,CH_2), 3.79 (s, 2H,CH_2), 3.14 (t, J = 8.7 Hz, 2H,OCH_2CH_2); ^{13}C NMR (151 MHz, $CDCl_3$) δ 167.39, 159.62, 144.77, 140.34, 139.55, 134.53, 134.10, 132.68, 131.89, 130.38, 129.92, 129.38, 128.42, 128.29, 128.14, 127.67, 127.45, 126.63, 124.53, 122.41, 109.08, 71.32, 49.50, 33.21, 32.96, 29.64; ESI-MS *m/z*: 503.1 $[M + H]^+$; m.p. 125.8-127.1°C.

4-(3,5-Difluorophenyl)-N-((2,3-dihydrobenzofuran-5-yl)methyl)-5-(2-methoxybenzyl)thiazol-2-amine ***(23)*** was obtained as a slight yellow solid in 78.0% yield. ^{1}H NMR(DMSO-d_6, 600 MHz) δ 3.15 (t, J = 8.4 Hz, 2H, -O-CH_2-CH_2-), 3.76 (s, 3H, OCH_3), 4.04 (s, 2H, CH_2), 4.32 (d, J = 5.4 Hz, 2H, -NH-CH_2-), 4.50 (t, J = 8.4 Hz, 2H, -O-CH_2-CH_2-), 6.70 (d, J = 8.4 Hz, 1H, ArH), 6.90 (t, J = 7.2 Hz, 1H, ArH), 7.01 (d, J = 8.4 Hz, 1H, ArH), 7.11-7.05 (m, 2H, ArH), 7.18 (t, J = 9.0 Hz, 1H, ArH), 7.24 (dd, J = 13.8, 6.6 Hz, 4H, ArH), 7.91 (t, J = 5.4 Hz, 1H, -NH-CH_2-); ^{13}C NMR (151 MHz, $CDCl_3$) δ 166.68, 163.64, 162.00, 159.74, 156.93, 129.54, 129.35, 128.07, 127.73, 127.53, 124.57, 121.93, 120.63, 111.29, 110.30, 109.18, 102.74, 102.57, 102.40, 77.23, 77.02, 76.80, 71.35, 55.15, 49.50, 29.62, 27.26; ESI-MS *m/z*: 465$[M + H]^+$; m.p.129.3-131.0℃.

Biology.

Cells and Plasmids. HEK 293T cells were obtained from the National Platform of Experimental Cell Resources for Sci-tech (Beijing, China). The pNL4-3.luc.R^-E^- plasmid was obtained from the National Institute of Health AIDS Research and Reference Reagent Program. VSVG plasmid was kindly provided by Dr. Lijun Rong (University of Illinois at Chicago). The pNL4-3 plasmids with RT mutations were constructed as described previously [19].

Anti-HIV Activity Assay by Pseudotyped Viruses. Vesicular stomatitis virus glycoprotein (VSVG) plasmid and env-deficient HIV vector (pNL4-3.luc.R^-E^- or pNL4-3.luc.$R^-E^-_{RT\text{-}mutant}$) [20,21]. were co-transfected into HEK 293T cells using the $Ca_3(PO_4)_2$ method [22]. The supernatant containing pseudotyped virions was collected and filtered through 0.22 μm filters 48 h post-transfection. The harvested viral solution was quantified using p24 concentrations using an ELISA kit (ZeptoMetrix, Cat.: 0801111) and diluted to 0.2 ng p24/mL.

HEK 293T cells were seeded on 24-well plates at a density of 6×10^4 cells/well one day prior to infection. The compounds were added to the target cells 15 min prior to infection. Cells were infected using VSV-G/HIV_{wt} or VSV-G/HIV_{mut} virus calculated to 0.2 ng p24/mL. Forty-eight hours post-infection, 293T cells were lysed, and the luciferase activity of the cell lysate was measured using a Sirius luminometer (Berthold Detection System) according to the manufacturer's instructions.**Cytotoxicity**. HEK 293T cells were seeded at a density of 1×10^4 cells/well in 96-well plates. The next day, serially diluted compounds were incubated with 293T cells and further cultured for 48 hours. The cytotoxicity was measured using a cell proliferation assay kit (Promega) according to the manufacturer's instructions.

RT RNA-Dependent DNA Polymerase Activity Detection. HIV-1 reverse transcriptase RNA-dependent DNA polymerase activity was detected as our previously described [23]. The tested compound was added into 60 μL reaction system containing 11.7 ng/L poly(rA), 11.7 ng/L oligo(dT)15, 2.8 μM dTTP, 800 nM Digoxigenin-11-dUTP, 40 nM Biotin-11-dUTP, 50 mM Tris-HCl (pH7.8), 290 mM KCl, 30 mM $MgCl_2$ and 10 mM DTT. The reaction was initiated by the addition of 0.226 ng/L RT followed by 1 h incubation at 37℃. Then the mixture was transferred into a streptavidin-coated plate (Roche) to incubate at 37℃ for 1 h. The supernatant was then removed and the plate was washed with PBS. Anti-DIG-POD was added to the plate and incubated at 37℃ for 1 h. Washed the plate and added

TMB (3,3,5,5-tetramethylbenzidine). Read OD_{450} values by a microplate reader (Molecular Devices).

Computational

Docking and 3D-QSAR. All of the reported calculations were performed on an HP Z800 workstation with Red Hat Enterprise Linux 5 operating system using the Tripos Sybyl-X 1.2 (Tripos Inc., St Louis, MO, USA) molecular modeling package. The parameters in the study were set to default values except for those specifically mentioned.

Acknowledgments

This work was supported by the National Natural Basic Research Program of China (No. 81273561 & 81473256), the National Science and Technology Major Project (No. 2015ZX09102-023-004) and the central level, scientific research institutes for basic R & D special fund business (No. 2015CX16).

Appendix A. Supplementary data

Supplementary data related to this article can be found at XXXX

References

1. G. Barbaro, A. Scozzafava, A. Mastrolorenzo, C.T. Supuran, Highly active antiretroviral therapy: current state of the art, new agents and their pharmacological interactions useful for improving therapeutic outcome, Curr. Pharm. Des. 11 (2005) 1805-1843. doi: 10.2174/1381612053764869.

2. D.D. Ho, A.U. Neumann, A.S. Perelson, W. Chen, J.M. Leonard, M. Markowitz, Rapid turnover of plasma virions and CD4 lymphocytes in HIV-1 infection, Nature 373 (1995) 123-126. doi: 10.1038/373123a0.

3. S.M. Hammer, D.A. Katzenstein, M.D. Hughes, H. Gundacker, R.T. Schooley, R.H. Haubrich, W.K. Henry, M.M. Lederman, J.P. Phair, M. Niu, M.S. Hirsch, T.C. Merigan A Trial Comparing Nucleoside, Monotherapy with combination therapy in HIV-infected adults with CD4 cell Counts from 200 to 500 per cubic millimeter. AIDS Clinical Trials Group Study 175, N. Engl. J. Med. 335 (1996) 1081-1090. doi: 10.1056/NEJM199610103351501.

4. R.M. Gulick, A. Meibohm, D. Havlir, J.J. Eron, A. Mosley, J.A. Chodakewitz, R. Isaacs, C. Gonzalez, D. McMahon, D.D. Richman, M. Robertson, J.W. Mellors, Six-year follow-up of HIV-1-infected adults in a clinical trial of antiretroviral therapy with Indinavir, zidovudine, and Lamivudine, AIDS 17 (2003) 2345-2349. doi: 10.1097/01.aids.0000076346.42412.97.

5. S.P. Goff, Retroviral reverse transcriptase: synthesis, structure, and function, J. Acq. Immun. Def. Synd. 3 (1990) 817–831.

6. J.J. DeStefano, R.G. Buiser, L.M. Mallaber, T.W. Myers, R.A. Bambara, P.J. Fay, Polymerization and RNase H activities of the reverse transcriptases from avian myeloblastosis, human immunodeficiency, and Moloney murine leukemia viruses are functionally uncoupled, J. Biol. Chem. 266 (1991) 7423–7431.

7. M. Harris, J.S. Montaner, Clinical uses of non-nucleoside Reverse transcriptase inhibitors, Rev. Med. Virol. 10 (2000) 217-229.

8. L.A. Sorbera, N. Serradell, E. Rosa, J. Bolós, Rilpivirine, Drugs Future 32 (2007) 1046-1052. doi: 10.1358/dof.2007.032.12.1159663.

9. Huang B.; Liang X.; Li C, et al. Fused heterocycles bearing bridgehead nitrogen as potent HIV-1 NNRTIs. Part 4: Design, synthesis and biological evaluation of novel imidazo[1,2-a]pyrazines. *Eur. J. Med. Chem*. **2015**, 93:330 – 337.

10. Huang B.; Li C.; Chen W, et al. Fused heterocycles bearing bridgehead nitrogen as potent HIV-1 NNRTIs. Part 3: Optimization of [1,2,4]triazolo[1,5-a]pyrimidine core via structure-based and physicochemical property-driven approaches. *Eur. J. Med. Chem.* **2015**, 92C:754-765.

11. Li W.; Li X.; Clercq E. D, et al. Discovery of potent HIV-1 non-nucleoside reverse transcriptase inhibitors from arylthioacetanilide structural motif. *Eur. J. Med. Chem.* **2015**, 102(44):167-179.

12. S.C. Piscitelli, C. Flexner, J.R. Minor, M.A. Polis, H. Masur, Drug interactions in patients infected with human immunodeficiency virus, Clin. Infect. Dis. 23 (1996) 685-693. doi: 10.1093/clinids/23.4.685.

13. M. Louie, M. Markowitz, Goals and milestones during treatment of HIV-1 infection with antiretroviral therapy: a pathogenesis-based perspective, Antiviral Res. 55 (2002) 15-25. doi: 10.1016/S0166-3542(02)00022-0.

14. D. Boden, A. Hurley, L. Zhang, Y. Cao, Y. Guo, E. Jones, J. Tsay, J. Ip, C. Farthing, K. Limoli, N. Parkin, M. Markowitz, HIV-1 drug resistance in newly infected individuals, JAMA 282 (1999) 1135-1141. doi: 10.1001/jama.282.12.1135.

15. F. Ceccherini-Silberstein, V. Svicher, T. Sing, A. Artese, M.M. Santoro, F. Forbici, A. Bertoli, S. Alcaro, G. Palamara, A. d'Arminio Monforte, J. Balzarini, A. Antinori, T. Lengauer, C.F. Perno, Characterization and structural analysis of novel mutations in Human immunodeficiency virus Type 1 reverse transcriptase involved in the regulation of resistance to nonnucleoside inhibitors, J. Virol. 81 (2007) 11507-11519. doi: 10.1128/JVI.00303-07.

16. Z.K. Sweeney, K. Klumpp, Improving non-nucleoside reverse transcriptase inhibitors for first-line treatment of HIV infection: the development pipeline and recent clinical data, Curr. Opin. Drug Discov. Devel. 11 (2008) 458-470.

17. D. Wang, W. Lu, F. Li, Pharmacological intervention of HIV-1 maturation, Acta Pharm. Sin. B 5 (2015) 493-499. doi: 10.1016/j.apsb.2015.05.004.

18. Z. Xu, M. Ba, H. Zhou, Y. Cao, C. Tang, Y. Yang, R. He, Y. Liang, X. Zhang, Z. Li, L. Zhu, Y. Guo, C. Guo, 2,4,5-Trisubstituted thiazole derivatives: a novel and potent class of non-nucleoside inhibitors of wild type and mutant HIV-1 reverse transcriptase, Eur. J. Med. Chem. 85 (2014) 27-42. doi: 10.1016/j.ejmech.2014.07.072.

19. Y.L. Cao, S.X. Li, H. Chen, Y. Guo, [Establishment of pharmacological evaluation system for non-nucleoside reverse-transcriptase inhibitors resistant HIV-1], Yao Xue Xue Bao 44 (2009) 355–361.

20. J. He, S. Choe, R. Walker, P. Di Marzio, D.O. Morgan, N.R. Landau, Human immunodeficiency virus Type 1 viral protein R (Vpr) arrests cells in the G2 phase of the cell cycle by inhibiting p34cdc2 activity, J. Virol. 69 (1995) 6705-6711.

21. R.I. Connor, B.K. Chen, S. Choe, N.R. Landau, Vpr is required for efficient replication of human immunodeficiency virus Type-1 in mononuclear phagocytes, Virology 206 (1995) 935-944. doi: 10.1006/viro.1995.1016.

22. L. Rong, P.J. Bates, Analysis of the Subgroup A avian sarcoma and leukosis virus receptor: the 40-residue, cysteine-rich, low-density lipoprotein receptor repeat motif of Tva is sufficient to mediate viral entry, J. Virol. 69 (1995) 4847-4853.

23. X. Ma, L. Li, T. Zhu, M. Ba, G. Li, Q. Gu, Y. Guo and D. Li, Phenylspirodrimanes with Anti-HIV Activity from the Sponge-Derived Fungus Stachybotrys chartarum MXH-X73[J], J NAT PROD, 76 (2013) 2298-2306.

List of Captions

Scheme 1. Synthesis of **3-23**.

Table 1. Chemical structures and cell-based antiviral activities of compounds **3-23**[a] against wild-type HIV-1

Table 2. Antiviral activities of compound 14, 16, 17 and 19 against wild-type HIV-1

Table 3. Inhibitory effects of **4**, **9**, **10**, **11**, **13**, **16** and the references NVP and EFV on wild-type and NNRTI-resistant HIV-1 replication, as determined through a cell-based antiviral assay

Figure 1. Structures and anti-HIV activities of compounds **1**, **2**, and **3**.

Figure 2. Binding conformation of **16** (magenta), **17** (white) and **19** (orange) into the NNBS of HIV-1WT RT (PDB id:2rki). Hydrogen bonds are shown as dotted yellow lines.